Check for updates

View Article Online
View Journal

Integrative Biology

Accepted Manuscript

This article can be cited before page numbers have been issued, to do this please use: N. Bourguignon, C. Attallah, P. Karp, R. Booth, A. Peñaherrera, C. Payés, M. Oggero, M. Pérez, G. Helguera and B. Lerner, *Integr. Biol.*, 2018, DOI: 10.1039/C7IB00200A.

This is an Accepted Manuscript, which has been through the Royal Society of Chemistry peer review process and has been accepted for publication.

Accepted Manuscripts are published online shortly after acceptance, before technical editing, formatting and proof reading. Using this free service, authors can make their results available to the community, in citable form, before we publish the edited article. We will replace this Accepted Manuscript with the edited and formatted Advance Article as soon as it is available.

You can find more information about Accepted Manuscripts in the author guidelines.

Please note that technical editing may introduce minor changes to the text and/or graphics, which may alter content. The journal's standard Terms & Conditions and the ethical guidelines, outlined in our author and reviewer resource centre, still apply. In no event shall the Royal Society of Chemistry be held responsible for any errors or omissions in this Accepted Manuscript or any consequences arising from the use of any information it contains.

ROYAL SOCIETY OF CHEMISTRY

rsc.li/integrative-biology

View Article Online
DOI: 10.1039/C7IB00200A

This paper attempt to be a significant contribution for the improvement of the quality of life through the development of a new and innovative methodology that uses microfluidic systems for the production of monoclonal antibodies, considered advanced pharmaceutical products for the treatment of autoimmune diseases. Thus, a revolutionary interdisciplinary method is intended to be developed from the microtechnological point of view. It has new insights and applicability at the same time, taking into account that monoclonal antibodies for therapeutic use have a great added value and also numerous applications which shows a high integration of the work. Because of this, it is believed that the proposed devices will provide great social and scientific benefits from the health point of view.

Published on 15 February 2018. Downloaded by University of Windsor on 16/02/2018 11:35:28.

Integrative Biology Accepted Manuscript

View Article Online
DOI: 10.1039/C7IB00200A

Journal Name

ARTICLE

Published on 15 February 2018. Downloaded by University of Windsor on 16/02/2018 11:35:28.

Production of monoclonal antibodies in microfluidic devices

Natalia Bourguignon[a]†, Carolina Attallah[b]†, Paola Karp[c]†, Ross Booth[d], Ana Peñaherrera[a], Cristian Payés[c], Marcos Oggero[b], Maximiliano Pérez[ae], Gustavo Helguera[c]* and Betiana Lerner[ae]*

Received 00th January 20xx,
Accepted 00th January 20xx

DOI: 10.1039/x0xx00000x

www.rsc.org/

Here is presented a microfluidic device with cisterns design for cultivation of adherent eukaryotic cells for the production of recombinant proteins. The geometric configuration of the microchannels in the device provided laminar flow with reduced velocity profiles in the cisterns, resulting in an adequate microenvironment for long term adherent cell growth with passive pumping flow cycles of 24 hours. CHO-ahIFNα2b and HEK-ahIFNα2b adherent cell lines expressing a novel anti-hIFN-α2b recombinant monoclonal antibody (MAb) for treatment of Systemic Lupus Erythematosus were cultured on the surface of PDMS/glass microchannels coated with poly-D-lysine. A 24-days culture of CHO-ahIFNα2b cells resulted in MAb concentrations up to 166.4 µg mL^{-1} per day. The productivity of CHO-ahIFNα2b and HEK-ahIFNα2b cell lines was higher in the microdevice compared to adherent cell culture method (T-flask), with a 5.89 and 7.31 fold increase, respectively. Moreover, biological analysis of the MAbs produced in the microdevice showed no significant differences in the neutralizing antiproliferative activity of the hIFN-α2b or the cytokine cell signaling compared to the MAbs produced with cell adherent methods. These results suggest that this microfluidic device is suitable for long term culture of mammalian cells and can improve the productivity of cells expressing recombinant MAbs with potential for therapeutic use without affecting quality attributes of the product.

Introduction

Microfluidics provides promising platforms for lab-on-a-chip (LOC) applications, including the use of microdevices for the culture of prokaryotic and eukaryotic cells, such as yeast and mammalian cells to produce recombinant proteins in microbioreactors[1–3]. Previous works have reported microfluidic platforms for the culture of mammalian cells[4], microreactors with oxygen control[5], and devices that allow the modeling of the *in vivo* environment at different cell level organizations[6]. They have been used also to perform cytotoxicity studies[7], enrichment of stem cells, use of co-culture systems to monitor tumor-stromal interactions on a chip[8], among other applications.

Microfluidic cell cultivation has been applied also to better understand bioprocess-related phenomena, to analyze cellular heterogeneity during cell population growth and to identify arresting cells and highly proliferating cells[3,9]. Moreover, the use of microfluidic devices for expression of recombinant proteins intended for therapeutic use, offers several advantages including higher surface/volume ratio, homogenous and controlled microenvironments, reduction in sample volumes, power requirements and manufacturing cost for process optimization[10]. Besides, they have shown increase of volumetric productivity for synthetic molecules, with better controlled environment and short residence time of the product in the device, minimizing the impact of unwanted chemicals or enzymatic modifications during the process[11].

The production of monoclonal antibodies (MAbs) for therapeutic use is one of the areas of fastest growth in the biopharmaceutical industry[12,13]. Since the first therapeutic MAb was commercialized in 1986, 47 MAbs were approved in the United States and Europe for the treatment of a variety of diseases, such as cancer and autoimmune diseases as of 2014. With the current approval rate of four new products per year, 70 commercial MAbs will be on the market and an estimated projection of combined global sales will be nearly $ 125 billion in 2020[14]. Since high levels of serum human interferon-α (hIFN-α) has been reported to be a hereditary risk factor for contracting Systemic Lupus Erythematosus (SLE)[15,16], a novel anti-hIFN-α recombinant antibody-like molecule (a single chain antibody variable fragment fused to the crystallizable domain of the human IgG1, scFv-Fc) was developed in our laboratory[17]

[a] Facultad Regional Haedo, Universidad Tecnológica Nacional (UTN), Provincia de Buenos Aires CP 1706, Argentina.
[b] Laboratorio de Cultivos Celulares, Facultad de Bioquímica y Ciencias Biológicas, Universidad Nacional del Litoral (UNL), CONICET, Santa Fe, Provincia de Santa Fe, 3000ZAA, Argentina.
[c] Laboratorio de Biotecnología Farmacéutica, Instituto de Biología y Medicina Experimental (IBYME CONICET), Ciudad de Buenos Aires C1428ADN, Argentina.
[d] MilliporeSigma Corporation, Hayward, CA 94545, USA
[e] Instituto de Ingeniería Biomédica, Universidad de Buenos Aires (UBA), Ciudad de Buenos Aires C1063ACV, Argentina.
* Corresponding authors
† Authors contributed equally to this work.
Electronic Supplementary Information (ESI) available: [details of any supplementary information available should be included here]. See DOI: 10.1039/x0xx00000x

Integrative Biology Accepted Manuscript

Please do not adjust margins
View Article Online
DOI: 10.1039/C7IB00200A

Published on 15 February 2018. Downloaded by University of Windsor on 16/02/2018 11:35:28.

and successfully expressed in an active form by CHO-K1 and HEK293 cells using *in vitro* adherent cell culture in T-flask. Here, this molecule was employed as a model to study the ability of on chip-immobilized cells to express functional recombinant proteins with potentially therapeutic uses.

One way to improve the control of the production of MAbs is to reduce the scale of the system by miniaturization in the form of microdevices. Until now, only one group has reported the production of antibodies in LOC devices[18]. They designed a chip with a polymethylmethacrylate (PMMA) base and a polydimethylsiloxane (PDMS) cover to produce the commercial MAb Infliximab™ as an alternative to traditional production using agitated tanks. These authors applied microdevices and reached antibody productivity values about three orders of magnitude higher than those typically reported in fed batch suspension cultures and achieved high cell density in the microchannels[1,18]. However, the authors proposed different microdevice geometries with small area available for cell proliferation with low shear/low vorticity resulting in non-homogeneous flow velocity distribution over the production cells. Moreover, non-homogeneous cell distribution was observed and generation of vortices in the flow were determined by flow modeling, which may have contributed to the limited time of production of 5 days[1,18].

In the present work a novel microfluidic system is proposed, comprised of microchannels with cisterns that prove an adequate microenvironment for the adhesion and growth of the MAb-producing cells. Flow simulation within the channels was performed and the production of anti-hIFN-α2b chimeric antibody was studied in two different cell lines. Finally, we conducted analysis of quality attributes of the product where the neutralizing ability of the MAb produced in the microdevice was compared with the MAb produced with the method of adherent cell culture in T-flasks, results that suggest the feasibility of production of recombinant proteins in microfluidic chips.

Experimental Methods

Microfluidic devices design and fabrication

The microfluidic devices used in this study were designed using the Layout Editor software. The microchip consists of an inlet and an outlet channel connected. The inlet channel divides into four identical microchannels (496 µm width) with 4 cisterns each (1690 µm width), after which the flows are reunited to a single chip outlet. The channel height is 150 µm, and the total internal volume is 32.22 µL (**Figure 1**). The channels were joined by curved wave channels to avoid the Corning). To do this, a mold of the design in high relief was made by photolithographically patterning 150 µm thick SU-8 accumulations of cells in straight corners and the formation of bubbles[9].

The microdevices were built in PDMS (Sylgard 184, Dow (MicroChem, Germany) on a silicon wafer (Virginia Semiconductor, Inc.). The silicon substrate was cleaned by

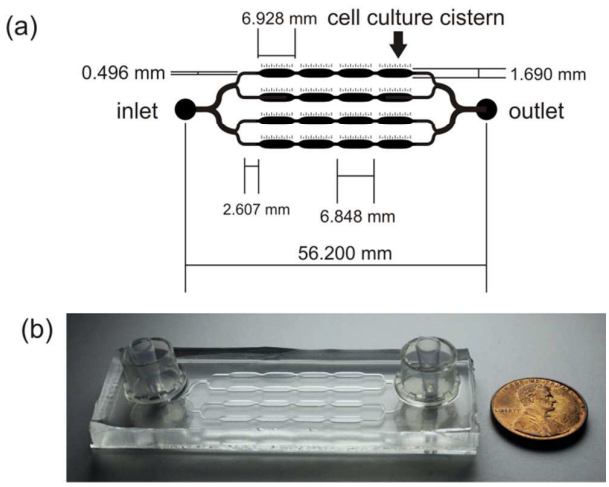

Figure 1. (a) Microchannels design with an inlet, an outlet and sixteen cell culture cisterns. (b) PDMS/glass microfluidic device with total internal volume of 32.22 µL.

sonication in acetone and isopropyl alcohol, and the substrate surface was dehydrated for 10 min on a hotplate at 200 °C. Then, SU-8 resin was dispensed on the substrate and spun in two identical cycles. To spread the resin, the spinner was ramped at 100 rpm s 1 to 500 rpm, and held for 5 s. In the spin cycle, the spinner was ramped at 300 rpm s 1 to 2000 rpm, and held for 30 s. The resin was soft baked at 65 °C for 20 min, then at 95 °C for 50 min. The substrate was aligned and the resin was exposed to near UV at 650 mJ cm 2. The resin was post-exposure baked at 65 °C for 12 min, then 95 °C for 15 min. Finally, the SU 8 resin was developed for 15 min under agitation.

PDMS was mixed with curing agent at 10:1 ratio. The mixture was placed under vacuum to remove air bubbles. After this, the mixture was poured into the master, placed under vacuum once again, and cured in an oven at 70 °C for 70 min (**Supplementary Figure S1**). Finally the device was cut and the fluidic connection ports were punched with a hollow punch (inner diameter 0.51 mm). The device was then irreversibly bonded to a glass wafer after exposure to a high frequency generator (BD 10AS, Chicago, USA) for 120 s.

Flow field characterization by computational flow modeling

To define predicted flow dynamic profiles of the microfluidic device, Comsol 5.2a software was used to simulate flow in the channel design perfused at the experimentally relevant flow rate of 3.28 $mm^3\ s^{-1}$. Computation was based upon the Navier-Stokes equations while neglecting the inertial component due to the very low Reynolds number of microfluidics devices, allowing for computation at a higher mesh density. Boundary conditions for the 3D model included no slip, laminar creeping flow, zero pressure at the outlet, and the fluid material properties of water. Mesh density was built to include >900,000 elements of freedom, with an average element quality of >0.6.

Integrative Biology Accepted Manuscript

This journal is © The Royal Society of Chemistry 20xx
Please do not adjust margins

View Article Online
DOI: 10.1039/C7IB00200A

Published on 15 February 2018. Downloaded by University of Windsor on 16/02/2018 11:35:28.

Cell culture and distribution

The surface of the microchannels was exposed to oxygen plasma for 3 min to modify the PDMS from hydrophobic to hydrophilic. Then, 70% ethanol was rinsed inside the microchannels because it has lower surface tension than water. After that, the microfluidic chip was disinfected using NaOH 0.5 M for 30 min, and then rinsed with 4 mL of sterile water. Before cell seeding, the chip was incubated with poly-D-lysine hydrobromide 0.1 mg mL^{-1} (Sigma, Saint Louis, USA) sterile solution for 30 min at 37 °C in order to improve the attachment of the cells. We used Chinese hamster ovary CHO-K1, CHO-ahIFNα2b and human embryonic kidney HEK-ahIFNα2b adherent cell lines. The last two cell lines expressing anti hIFN-α2b recombinant scFv-Fc molecules were generated by transfection and subsequent puromycin selection as previously described[17]. The scFv sequence was obtained as described by Depetris et al.[19] and modified by adding mSA signal peptide to allow the scFv-Fc being expressed in mammalian cells as described by Attallah et al. [17]. The scFv-Fc sequence was obtained by the fusion of the human-Fcγ1 sequence to the previously generated scFv. The Fcγ1 was synthesized by GeneArt™ Gene Synthesis (Thermo Fisher Scientific, Waltham, MA, USA) and cloned between NheI and BamHI restriction sites in a pLV vector.

CHO-ahIFNα2b and HEK ahIFNα2b cells were maintained in adherent cell culture in flasks with 50/50% mixture of F 12/DMEM growth media (Gibco, Waltham, MA, USA) supplemented with fetal calf serum heat-inactivated fetal bovine serum (FBS) 10% (w/v) (Internegocios, Mendoza, Argentina), gentamicin 50 µg mL^{-1} (Invitrogen, Grand Island, NY, USA). $NaHCO_3$ 2.44 g L^{-1} (F12/DMEM) and 1.5 g L^{-1} (DMEM); and only DMEM was supplemented with sodium pyruvate 0.11 g L^{-1}. The media for antibody production was the same, but supplemented with 0.5% FBS. The cells were resuspended with trypsin 0.5 mg mL^{-1} and EDTA-4Na 0.2 mg mL^{-1} (Gibco, New York, USA), and incubated at 37 °C for 3 min. Trypsin was then inactivated with FBS and the cells were washed with phosphate buffer solution (PBS: NaH_2PO_4 2.96 mM, KH_2PO_4 1.06 mM, NaCl 155 mM, pH 7.4) and centrifuged at 1000 rpm for 5 min. Prior to experiments, the cells were harvested and resuspended in fresh media, and cell numbers and viability were quantified using a Neubauer Chamber and trypan blue exclusion (Invitrogen, Grand Island, NY, USA). Next, mammalian cells in suspension were seeded into the syringe needle in the inlet of the microfluidic device at a concentration of $2x10^5$ cells per mL. The cells were allowed to settle and the microfluidic device was incubated inside a Petri dish at 37 °C in humidified incubator with 5% CO_2 for 3 days until cell adhesion is achieved on the floor of the microchip. Then, devices were fed with production culture medium which was renewed every two days. In all the conditions, being incubated in the same conditions

Cell growth measurement by image analysis

The microchannels were visualized using an inverted Olympus microscope CKX41 (Olympus, Tokyo, Japan). Bright field images were taken with Olympus objectives LUCPlan FLN 40X/0.60; LCAch N 20X/0.40; PlanC N 10X/0.25; and PlanC N 4X/0.10 with an Olympus QColor 5; and processed with QCapture Pro 6.0 software.

A total of 16 micrographs of the microdevice were taken per day, one for each cistern at a 100X magnification in clear field during the cell proliferation experiment. Cell numbers (with distinguishable nuclei) and densities per mm^2 were determined using ImageJ (US National Institutes of Health, http://rsb.info.nih.gov/ij/). For quantification, each photomicrograph was divided into 24 of 0.38 mm^2 or 16 of 0.57 mm^2 equal quadrants, depending on the assay, thus an automatic macro for all photographs was created to quantify cells of each area with the ImageJ cell counter plugin. From measurements at each specific cistern, the average number of new cells per quadrant on the microchip per day was determined.

Monoclonal antibody quantification

Indirect ELISA was performed in 96 well plates (Greiner Bio One, Kremsmünster, Austria). Coating was achieved by incubating the plates with 50 ng per well of a rhIFN-α2b solution in 50 mM carbonate/bicarbonate buffer (pH 9.6) for 1 h at 37 °C and then ON at 4 °C. After blocking 1 h at 37 °C with 1% (w/v) bovine serum albumin (BSA) in phosphate-buffered saline (PBS: Na_2HPO4 10 mM, KH_2PO_4 1.8 mM, NaCl 14 mM, KCl 2.7 mM, pH 7.4), plates were incubated with 2 fold serial dilutions of the chimeric protein standard (mentioned below) or the test samples for 1 h at 37 °C. Then, plates were incubated with an appropriately diluted polyclonal rabbit anti human immunoglobulin (DAKO, Denmark) for 1 h at 37 °C. Finally, horseradish peroxidase (HRP) labeled polyclonal goat anti rabbit immunoglobulin (DAKO, Denmark) diluted 1:2,000 were added to the wells. After 1 h incubation, plates were incubated for 10 min with substrate solution (3 mg mL^{-1} o phenylenediamine, 0.12% (v/v) H_2O_2 in 50 mM phosphate citrate buffer). Absorbance was measured at 492 nm with a microtiter plate reader (Labsystems Multiskan MCC/340, Finland). Between every step, plates were washed 6 times with PBS containing 0.05% (v/v) Tween 20 (PBS-T). Dilutions of tested samples and antibodies were prepared in PBS-T containing 0.1% (w/v) BSA. Protein A affinity-purified scFv-Fc was used as standard to prepare a 2 fold serial dilution curve from 1,000 ng mL^{-1} to 7.8 ng mL^{-1}. The assay was reproduced by triplicate.

Evaluation of MAb quality attributes

The antiproliferative activity of rhIFN-α2b is routinely determined by measurement of its ability to inhibit the growth of Daudi cells[20]. Contrarily, the neutralizing effect of the antibodies was evaluated as the ability to allow the cell growth. Serial 1:2 dilutions of anti-rhIFN-2αb containing supernatant were pre-incubated for 2 h at 37 °C with equal volume of 20 U mL^{-1} of rhIFN-α2b into microtiter plate wells. After that, previously washed Daudi cells were added ($1×10^4$ cells per well) and plates were incubated at 37 °C for 96 h. Cell proliferation was determined using a CellTiter 96TM AQueous Non Radioactive Cell Proliferation Assay (Promega,

Integrative Biology Accepted Manuscript

View Article Online
DOI: 10.1039/C7IB00200A

Published on 15 February 2018. Downloaded by University of Windsor on 16/02/2018 11:35:28.

Madison, WI, USA). Absorbance values were read at 492 nm using a microplate reader and plotted against scFv-Fc concentrations to determine the IC50 (antibody concentration necessary to inhibit the 50% of the maximum antiproliferative activity of the cytokine). The assay was reproduced in triplicate.

The concentration of scFv-Fc in supernatants was determined by specific indirect ELISA. For that, Protein A affinity purified scFv-Fc was used as standard to prepare a 2 fold serial dilution curve from 2,500 ng mL^{-1} to 19.5 ng mL^{-1}.

To evaluate the neutralization of biological activity of rhIFN−α2b cell signaling, HeLaMx2/eGFP reporter cells[21] were seeded in 96-well plates (1×10^4 cells per well) and incubated for 24 h at 37 °C with 5% CO_2. Supernatants of Hela cell culture were discarded and serial 1:2 dilutions of anti−rhIFN−α2b containing supernatant were added and pre-incubated for 2 h at 37 °C with equal volume of 50 U mL^{-1} of rhIFN−α2b. The cells were incubated for 24 h at 37 °C with 5% CO_2 and then trypsinized, carefully suspended in 0.2 mL PBS and finally eGFP expression was measured by flow cytometry. The concentration of scFv−Fc in supernatants was determined by specific indirect ELISA. For that, Protein A affinity-purified scFv−Fc was used as standard to prepare a 2−fold serial dilution curve from 5,000 ng mL^{-1} to 39.1 ng mL^{-1}. The sample concentrations were determined by indirect ELISA. Flow cytometry was performed on a Guava® Easy CyteTM cytometer (MilliporeSigma, Hayward, USA). This cytometer has a 488 nm blue laser for access to commonly used fluorescent dyes, and detectors to measure five different parameters (3 fluorescent channels and 2 light scatters). It allows simultaneous measurement of the side scatter (SSC), the forward scatter (FSC) and the green, yellow and red fluorescent emission which are collected by using the optical filters 525/30 nm, 583/26 nm and 690/50 nm, respectively. In addition, this equipment can measure samples from 96−well plates. Data acquisitions and analysis were performed using Guava CytoSoftTM 3.6.1 software. For each sample 5,000 events were collected gating on the FSC vs SSC dot plot. Flow calibration and optical alignment were performed with the aid of Flow−Check Fluorospheres (Guava® Check kit MilliporeSigma, Hayward, USA) before each determination. Cells were evaluated for the eGFP signal (means fluorescence intensity multiplied by percentage of eGFP positive cells) that is highly proportional to mRNA levels[22]. Data is representative of three independent experiments.

Results and discussion

Computational flow modelling

The geometric configuration of the microchannel design proposed here was planned to provide an optimally homogenous flow velocity across the cell culture surface in each of the four parallelized series of cisterns (**Figure 2**). The inlet channel divides into four microchannels with cisterns, after which the flows are reunited to a single chip outlet.

Passive pumping gravity-driven flow method was used in our open microfluidic system, generating the flow by reservoir height difference[23,24]. A similar strategy has been used by Ruiz et al.[25] showing that they could culture different populations of primary central nervous system (CNS) cells in an open multichannel configuration microfluidic chips. Under this configuration they could mimic physiological fluidic conditions and observe improved reproducibility of the cell density during plating, since the number of cells per chamber could be accurately controlled.

The calculated flow velocities and shear stress (**Figure 2a, 2b and Supplementary S1**) show areas of reduced flow (blue areas) in the cisterns with a proper environment for cell growth, allowing the generation of a continuous cell monolayer (**Figure 2c and 2d**). Although we observe lower velocity profiles in the cisterns compared to the channels (**Figure 2e**), it has been reported that general laminar flow ensures consistent diffusive mass transport that may result in a uniform microenvironment for cell growth[23]. In order to evaluate whether the seeded cells grow homogeneously distributed in the cisterns at 7 days, we used an imaginary grid to separate in quadrants the cisterns, counted the number of cells in them and determined average and standard deviation (**Figure 2e and 2f**). As expected, statistical analysis comparing the density of cells in the quadrants in different cisterns in the chip showed that no significant difference in cell distribution was observed (**Supplementary Table S1**). In contrast, other studies using zigzag and donut shaped cell culture microchannel configurations resulted in flow vortexing and inhomogeneous cell distribution[18], suggesting that the more homogeneous laminar flow in our system design may contribute in microchannel cell surface occupancy.

Studies have shown that continuous flow could affect the morphology and cellular structure of adherent cells, leading to a heterogeneous growth[26]. In order to minimize the stress on cultured cells, instead of continuous flow, we adopted a periodic media exchange protocol with pulsed cycles at 24 h intervals. This allows a sufficient residence time of the factors released by the cells that favor stability, growth and cell-cell communication. At the same time, the pulsed media flow provides the required nutrients and removes the building up of metabolic byproducts[26].

Cell growth and monoclonal antibody production

Adherent cells cultured on glass or plastic surfaces usually require a charged hydrophilic coating to encourage extracellular matrix cross-linking, which is necessary for cell attachment and expansion[4]. Our previous studies have shown that coating microchannels with poly-D-lysine promotes properly the cell adhesion to the floor of the microfluidic device[9]. To establish the optimal conditions for cell culture in the device, we cultured CHO-K1 cells and studied its proliferation in a long term culture by analysis of images obtained by bright field microscopy (**Figure 3a and**

Integrative Biology Accepted Manuscript

This journal is © The Royal Society of Chemistry 20xx

View Article Online
DOI: 10.1039/C7IB00200A

Published on 15 February 2018. Downloaded by University of Windsor on 16/02/2018 11:35:28.

Integrative Biology Accepted Manuscript

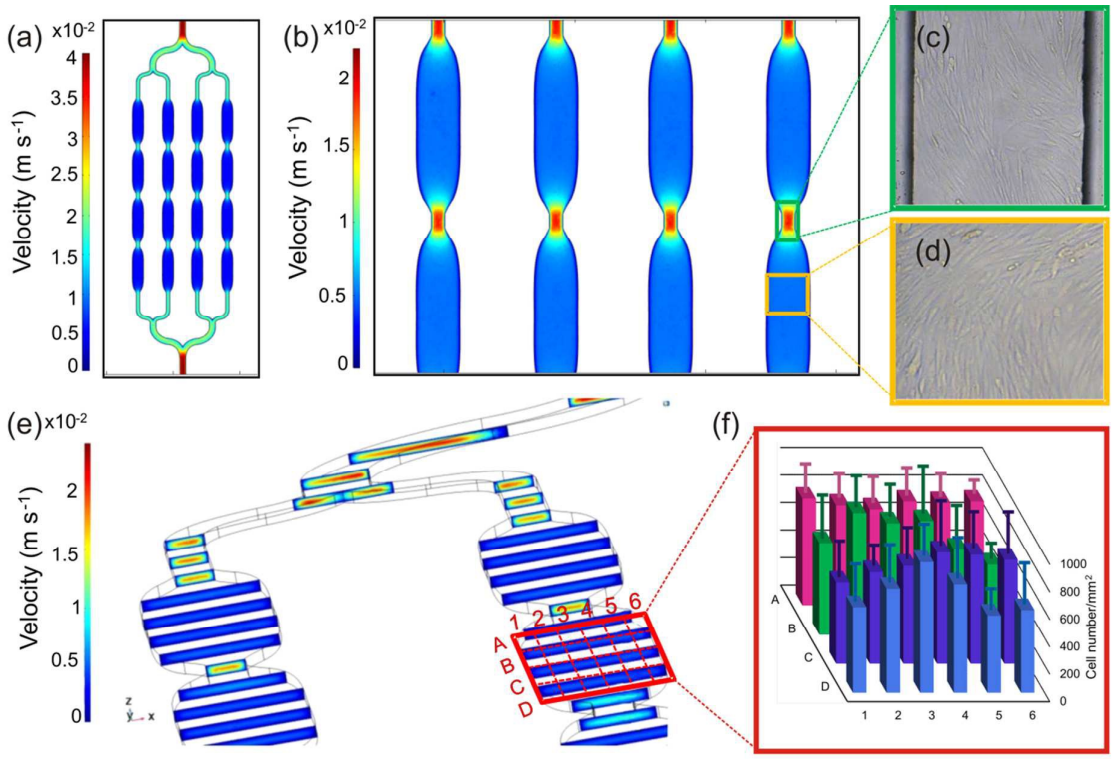

Figure 2. (a,b) Maximum velocity magnitude (m s^{-1}) at 75 µm height from a 3D simulation (Comsol 5.2a). CHO-K1 cells proliferation in microdevices in (c) microchannel connector and (d) cistern after 7 days of incubation. (e) Velocity magnitude in 3D microchannels simulation and (f) average cell number distribution in quadrants from four cisterns. Error bars indicate standard error of mean (SEM).

Supplementary Figure S3). The microdevices coated with poly-D-lysine were seeded at an initial concentration of $2x10^5$ cells per mL showing a wide range of diameters (between 12.2 and 22.5 µm) after cell attachment on the floor. The images indicate that the cells changed from their spherical morphology characteristic of suspension cultures observed at day 1, to propagation morphology from day 3 with appearance of borders suggesting a strong adhesion to the floor in monolayer type arrangement (**Figure 3a**).

Cell morphology is an important characteristic of adherent cell and is a major determinant of cell growth and function[27]. The number of cells per mm^2 vs. time of growth was determined by images analysis (**Figure 3a**). A slow growth of the CHO-K1 cells was observed in the microdevices during the first 48 h, this may be due to the time of adaptation to the new system that the cells need. From day 3 to 7 was observed a log proliferation with a growth rate of 0.0148 h^{-1} and 46.82 h of time of duplication (R^2=0.99). After 7 days of culture with daily changes of media, the cells reached almost 100% of confluence in the cisterns (**Figure 3a**). The cells exhibited a monolayer arrangement up to day 21 of culture, at which time the formation of clusters of detached cells from the substrate was first visualized. From day 24 to day 30 the number of cells decreased, and at day 31 a significant fraction of the cells were washed from the system. Those that remained within the microchannels presented signs of cellular stress showing a spherical shape and a disorganized cytoskeleton. Then, from day 35 to day 41 of culture the cells began to cover the surface again, to form a monolayer at day 44.

At day 49, signs of stress and loss of cell adhesion to the surface were observed, while at the time that the culture was ended at day 69, few new cells adhered, distributed, and grew

View Article Online
DOI: 10.1039/C7IB00200A

showing the morphological traits of viable cells, including oriented surface extension, cell body elongation and adherence to the substrate[28] (**Figure 3a**). These results demonstrate that the microdevice provides a microenvironment adequate for cell growth and proliferation; additionally, the system is suitable to sustain successive cycles of cell culture for a prolonged period without the need for a new inoculation, which allows continuous culture with the same inoculum without need to vary the passage. In contrast, previous studies with culture in microdevices in continuous perfusion achieved no more than 5 days of culture[18].

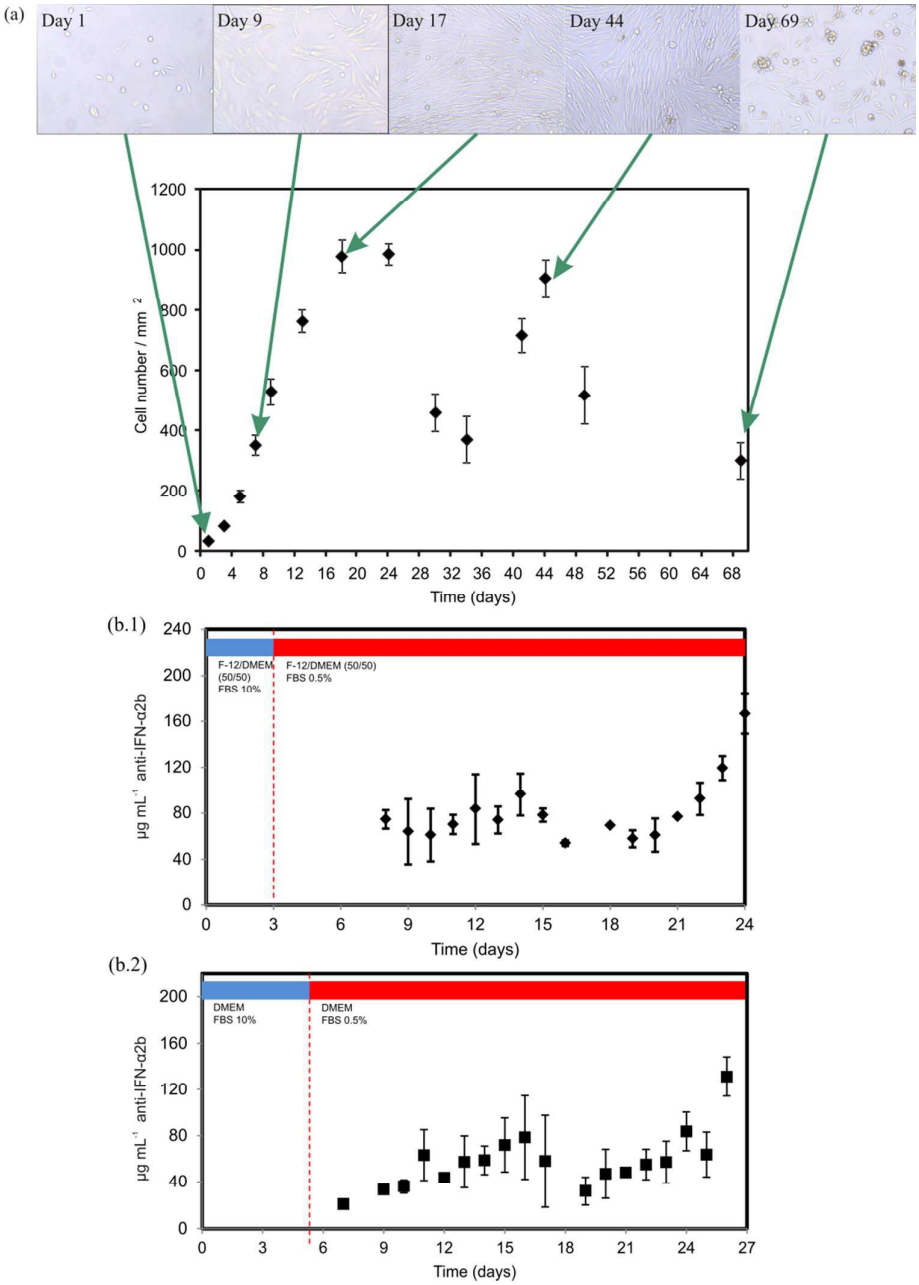

Figure 3. (a) Change in cell density of CHO-K1 cells cultured for 69 days in the microdevice. On top are shown bright field microscopy images (10X magnifications) of the CHO-K1 cells attached to the microchannel cisterns. (b) Average concentration level of MAb anti-hIFN-α2b harvested in 24 hour cycles of periodic media exchange of (b.1) CHO-ahIFNα2b and (b.2) HEK-ahIFNα2b cell lines cultured in the microdevices. Error bars indicate SEM determinations of three independent experiments.

This journal is © The Royal Society of Chemistry 20xx

Published on 15 February 2018. Downloaded by University of Windsor on 16/02/2018 11:35:28.
Integrative Biology Accepted Manuscript
Please do not adjust margins

View Article Online
DOI: 10.1039/C7IB00200A

Published on 15 February 2018. Downloaded by University of Windsor on 16/02/2018 11:35:28.

After establishing that CHO-K1 cells could be cultured in the microdevices, we evaluated the cultures of two cell lines expressing the chimeric antibody anti-hIFN-α2b, which entails a potential application for the therapy of autoimmune diseases[17]. CHO-ahIFNα2b and HEK-ahIFNα2b cell lines were cultured in devices by triplicate, under the same culture conditions previously tested. Both cell lines were cultured in the growth medium for 3 and 5 days, until reaching almost 100% of confluence. Next, the growth medium was shifted to the production medium, and samples collected from the device outlet to determine the concentration of functional antibodies by indirect specific ELISA. In addition, a western blot analyses was performed to identify the MAb in the microdevices samples and to compare with MAb produced by standard methods (**Supplementary Figure S4**). **Figure 3b** shows the daily production of anti-hIFN-α2b by CHO-ahIFNα2b (**Figure 3b1**) and HEK-ahIFNα2b (**Figure 3b2**) for 24 days. In the first two days the secreted MAb concentration increased to approximately 6.4 μg mL^{-1} for CHO-ahIFNα2b and 3.33 μg mL^{-1} for HEK-aIFNα2b, time at this both cell lines reached a MAb expression plateau. Subsequently, the production increased again from day 19 until the end time of the culture. During the production culture phase, a progressive increase in cell stress signals was observed in the cells morphology, which is expected due to the reduced concentration of FBS in the production culture medium. This may affect cell growth and proliferation, moreover when cell metabolism is mainly based in the production of the antibody.

Our studies showed that the average concentration of the MAb produced by CHO-ahIFNα2b was higher than in HEK-ahIFNα2b and the maximum value (166.4 μg mL^{-1}) was reached by CHO-ahIFNα2b on the last day of culture (**Figure 3b.1 and b.2** day 24). It is important to note that adherent cell cultures in T-flasks showed also significantly higher expression levels of MAb produced by CHO than HEK cell line[17].

Garza-García et al.[18] reported that the highest concentration of MAb produced in a microchip with a configuration of donut shaped chamber series was 7.2 μg mL^{-1} with residence times less than one minute constant flow, being the rates of production of 3 orders of magnitude higher than those observed in fed-tank bioreactors using suspended cells. In comparison, our system reached a maximum MAb concentration value 23 times greater than that reported by Garza-García et al.[18], with average production values (**Table 1**) between 11 and 7 times higher than those reported by these authors.

The average production of anti-hIFN-α2b observed in the microchips using both cell lines was superior compared to that obtained in T-flasks run in parallel, with values 1.36 and 1.70 times higher in CHO-ahIFNα2b and HEK-aIFNα2b, respectively (**Table 1**). Moreover, the overall productivity in picograms of anti-hIFN-α2b per cell and the productivity per day determined in the microchips using both cell lines was greater compared to that obtained in T-flasks run in parallel, with values 5.89 and 7.31 fold higher in CHO-ahIFNα2b and HEK-aIFNα2b, respectively. These results suggest that there are advantages in culturing adherent cells in the microdevices, showing increase in the yield of the product for longer period of time compared to higher scales culture conditions.

The advantage of producing MAb with adherent cell culture in microchips can be explained because microfluidic devices exhibit a high surface/volume ratio, many times higher than standard cell culture plates, leading to more efficient nutrient supply and avoiding dilution of secreted molecules. The volumes of the medium in nanoLiters and the very low cell-to-cell volume ratio are the factors that characterize both the microchannels of the devices and the cellular microniches *in vivo*[6]. One concern regarding the use of microdevices is the stability and robustness of the culture system over extended periods of operation for pilot (or commercial) production of biopharmaceuticals[18]. A previous report on the production of MAb in microchips showed a maximal culture time of 5 days[18]. In contrast, here we show that cell culture in the microdevice can run for 69 days and that different cell lines expressing a novel therapeutic MAb can be cultured at least for 24-days, achieving significantly better concentrations than the standard culture conditions. These results support the feasibility of continuous operation of the system in the long term, and therefore, its potential use in pilot scale production.

Evaluation of MAb quality attributes

A major concern to adopt an innovative system for the production of biotherapeutics is whether the process can

Table 1. Average of MAb production, MAb productivity and MAb productivity per day of CHO-ahIFNα2b and HEK-ahIFNα2b cell lines in microchips and T-flasks.

Cell line	Average MAb production			MAb productivity			MAb productivity per day		
	Microchip (μg mL^{-1})	T-flasks (μg mL^{-1})	ratio (microchips /T-flasks)	Microchip (pg $cell^{-1}$)	T-flasks (pg $cell^{-1}$)	ratio (microchips /T-flasks)	Microchip (pg $cell^{-1}$ day^{-1})	T-flasks (pg $cell^{-1}$ day^{-1})	ratio (microchips /T-flasks)
CHO-ahIFNα2b	81.22	59.46	1.36	1120.28	118.92	9.4	70.02	11.89	5.89
HEK-ahIFNα2b	54.72	32.27	1.70	754.76	64.54	11.7	47.17	6.45	7.31

Integrative Biology Accepted Manuscript

View Article Online
DOI: 10.1039/C7IB00200A
ARTICLE Journal Name

Published on 15 February 2018. Downloaded by University of Windsor on 16/02/2018 11:35:28.

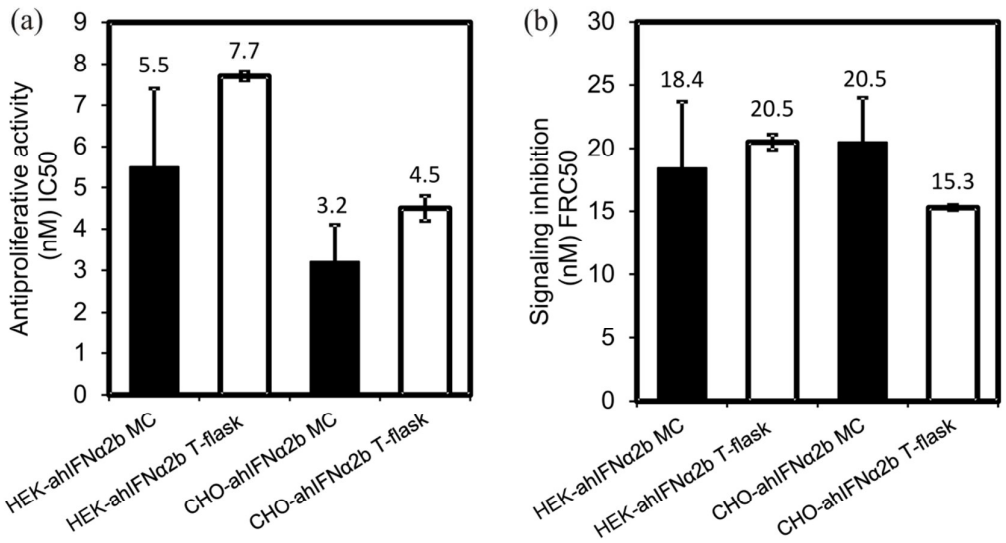

Figure 4. Evaluation of MAb quality attributes produced in the microdevice and T-flasks. (a) Antiproliferative activity inhibition measured as MAb concentration necessary to reduce 50% of the maximum cytokine potency (IC50) using Daudi cells. (b) Signalling inhibition measured as MAb concentration necessary to reduce 50% of the fluorescence (FRC50) using HelaMx2/eGFP cells. MC: production in microdevice. The error bar represents the SEM.

replicate the biological properties of the molecule of reference. To address this issue, we tested MAb quality attributes, specifically the MAb ability to neutralize the IFN-antiproliferative activity or the IFN-signaling by the action of the molecule produced in the microdevice compared to the one produced by the same cell lines using the adherent cell method in T-flasks.

Figure 4a shows a bar graph depicting the antibody concentration necessary to inhibit 50% of the antiproliferative activity of the cytokine (IC50) when Daudi cells were incubated with the antibody produced by HEK-ahIFNα2b and CHO-ahIFNα2b using the microdevice (MC) or the adherent cell culture method. The IC50 of the antibodies produced in microchips was not significantly different ($p<0.05$) to the IC50 of the antibodies produced in T-flasks as determined by ANOVA followed by Turkey's test.

Also, the attribute of the MAb to neutralize the hIFN-signaling was determined by fluorescence analysis using reporter cells whose eGFP expression is mediated by the hIFN-α2b inducible Mx promoter. **Figure 4b** shows a signaling inhibition bar graph corresponding to the concentration necessary to reduce 50% of the fluorescence (FRC50) measured by flow cytometry of the antibody produced by HEK-ahIFNα2b and CHO-ahIFNα2b using the MC or T-flasks. As in the previous experiment, the FRC50 of the antibodies produced by both cell lines using both procedures did not exhibit significant differences ($p<0.05$, Turkey's test). To the best of our knowledge, this is the first time that the quality attributes of biotherapeutics produced in microfluidic devices is tested in parallel with those produced by adherent cell culture in T-flasks. These results suggest that the production in microfluidic devices does not alter significantly the biological function of the antibodies in terms of their binding and neutralizing ability of the cytokine, compared to those produced with traditional adherent cell culture method.

Conclusions

Here we presented proof-of-concept for a microfluidic device with sequential cisterns design for adherent mammalian cell culture with periodic media exchange to express recombinant proteins. The computational simulation of the flow velocity in the microchannels of the designed device showed uniform distribution of the fluid. Also, quantification of CHO-K1 cells in the different domains of the device established homogeneous cell distribution, evidencing optimal conditions for adhesion and cellular growth. Interestingly, cells could be cultured in the device for more than two months.

Adherent CHO-ahIFNα2b and HEK-ahIFNα2b cells, expressing an anti-hIFN-α2b MAb as therapeutic candidate, were cultured in the microfluidic devices, achieving productivities 5.89 and 7.31 higher, respectively, than those obtained with *in vitro* adherent cell cultures in T-flasks. Moreover, the quality attributes of the MAb produced in the microchips showed no significant differences compared to the antibody produced with higher scale methods, suggesting that the system is suitable and may be advantageous for the development of MAb intended for therapeutic use.

Integrative Biology Accepted Manuscript

This journal is © The Royal Society of Chemistry 20xx

View Article Online
DOI: 10.1039/C7IB00200A

Published on 15 February 2018. Downloaded by University of Windsor on 16/02/2018 11:35:28.

Conflicts of interest

There are no conflicts to declare.

Acknowledgements

N.B., C.P., P.K. and A.B.P. are supported by Consejo Nacional de Investigaciones Científicas y Técnicas CONICET fellowships, G.H. is funded partially by Fundación Bunge y Born, Fundación Williams, and Fundación René Barón. C.A., M.O., M.P, B.L. and G.H. are members of CONICET. This work was supported with financial grants from CONICET (PIP2015), ANPCyT (PICT-STARTUP 3772), UNL-CAID (PI 50420150100006LI, PJ 50020110100045LI) and Florencio Fiorini Fundation. The authors would like to thank Gustavo Rosero for general support and discussion.

Notes and references

1 L. D. Garza-García, L. M. Carrillo-Cocom, D. Araiz-Hernández, P. Soto-Vázquez, J. López-Meza, E. J. Tapia-Mejía, S. Camacho-León, E. García-López, C. A. Rodríguez-González and M. M. Alvarez, *Lab Chip*, 2013, **13**, 1243-1246.
2 N. J. Mozdzierz, K. R. Love, K. S. Lee, H. L. T. Lee, K. A. Shah, R. J. Ram and J. C. Love, *Lab Chip*, 2015, **15**, 2918–2922.
3 T. Ladner, A. Grünberger, C. Probst, D. Kohlheyer, J. Büchs and F. Delvigne, *Application of Mini- and Micro-Bioreactors for Microbial Bioprocesses*, Elsevier B.V., 2016.
4 I. Barbulovic-Nad, S. H. Au and A. R. Wheeler, *Lab Chip*, 2010, **10**, 1536.
5 H. E. Abaci, R. Devendra, Q. Smith, S. Gerecht and G. Drazer, *Biomed. Microdevices*, 2012, **14**, 145–152.
6 K. Ziółkowska, R. Kwapiszewski and Z. Brzózka, *New J. Chem.*, 2011, **35**, 979.
7 K. Ziolkowska, E. Jedrych, R. Kwapiszewski, J. Lopacinska, M. Skolimowski and M. Chudy, *Sensors Actuators, B Chem.*, 2010, **145**, 533–542.
8 N. V. Menon, Y. J. Chuah, S. Phey, Y. Zhang, Y. Wu, V. Chan and Y. Kang, *ACS Appl. Mater. Interfaces*, 2015, **7**, 17095–17103.
9 A. Peñaherrera, C. Payés, M. Sierra-Rodero, M. Vega, G. Rosero, B. Lerner, G. Helguera and M. S. Pérez, *Microelectron. Eng.*, 2016, **158**, 126–129.
10 M. Jang, Y. J. Kwon and N. Y. Lee, *RSC Adv.*, 2015, **5**, 100905–100911.
11 S. J. Haswell, R. J. Middleton, B. O'Sullivan, V. Skelton, P. Watts and P. Styring, *Chem. Commun.*, 2001, 391–398.
12 IMARC Group, *IMARC report, SKU IMRC4880703* 2012.
13 A. A. Shukla and J. Thömmes, *Trends Biotechnol.*, 2010, **28**, 253–261.
14 D. M. Ecker, S. D. Jones and H. L. Levine, *MAbs*, 2015, **7**, 9–14.
15 K. A. Kirou and E. Gkrouzman, *Clin. Immunol.*, 2013, **148**, 303–312.
16 T. B. Niewold, J. Hua, T. J. A. Lehman, J. B. Harley and M. K. Crow, *Genes Immun.*, 2007, **8**, 492–502.
17 C. Attallah, M. Etcheverrigaray, R. Kratje and M. Oggero, *Protein Expr. Purif.*, 2017, **132**, 27–33.
18 L. D. Garza-García, E. García-López, S. Camacho-León, M. del Refugio Rocha-Pizaña, F. López-Pacheco, J. López-Meza, D. Araiz-Hernández, E. J. Tapia-Mejía, G. Trujillo-de Santiago, C. A. Rodríguez-González and M. M. Alvarez, *Lab Chip*, 2014, **14**, 1320-1329.
19 M. Depetris, P. Casalis, R. Kratje, M. Etcheverrigaray and M. Oggero, *J. Immunol. Methods*, 2008, **334**, 104–113.
20 T. Nederman, E. Karlström and L. Sjödin, *Biologicals*, 1990, **18**, 29–34.
21 M. Bürgi, C. Prieto, M. Oggero, M. Bollati-Fogolín, M. Etcheverrigaray and R. Kratje, *BMC Proc.*, 2011, **5**, P4.
22 A. Paillusson, N. Hirschi, C. Vallan, C. M. Azzalin and O. Mühlemann, *Nucleic Acids Res.*, 2005, **33**, 1–12.
23 M. Huang, S. Fan, W. Xing and C. Liu, *Math. Comput. Model.*, 2010, **52**, 2036–2042.
24 J. Shemesh, I. Jalilian, A. Shi, G. Heng Yeoh, M. L. Knothe Tate and M. Ebrahimi Warkiani, *Lab Chip*, 2015, **15**, 4114–4127.
25 A. Ruiz, P. Joshi, R. Mastrangelo, M. Francolini, C. Verderio and M. Matteoli, *Lab Chip*, 2014, **14**, 2860-2866.
26 E. Azuaje-Hualde, M. García-Hernando, J. Etxebarria-Elezgarai, M. De Pancorbo, F. Benito-Lopez and L. Basabe-Desmonts, *Micromachines*, 2017, **8**, 166.
27 N. Jaccard, L. D. Griffin, A. Keser, R. J. Macown, A. Super, F. S. Veraitch and N. Szita, *Biotechnol. Bioeng.*, 2014, **111**, 504–517.
28 B. Zhu, Q. Lu, J. Yin, J. Hu and Z. Wang, *J. Biomed. Mater. Res.*, 2004, **70B**, 43–48.

Integrative Biology Accepted Manuscript

Perfusion microfluidic device to culture adherent eukaryotic cells for the production of monoclonal antibodies with potential for therapeutic use.

View Article Online
DOI: 10.1039/C7IB00200A

Published on 15 February 2018. Downloaded by University of Windsor on 16/02/2018 11:35:28.

Integrative Biology Accepted Manuscript

View Article Online
DOI: 10.1039/C7IB00200A

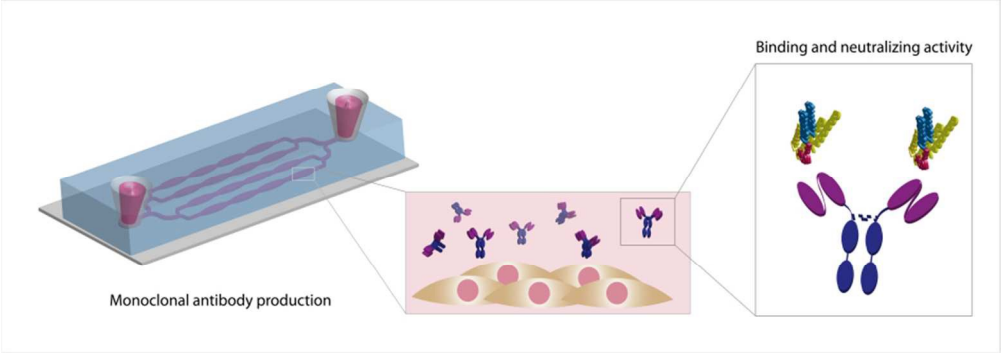

79x28mm (300 x 300 DPI)

Published on 15 February 2018. Downloaded by University of Windsor on 16/02/2018 11:35:28.

Integrative Biology Accepted Manuscript